LAWRENCE LIVERMORE NATIONAL LABORATORY

LLNL-CONF-642082

Fourier Transform Rheology of Paste Explosives: I. Semtex Formulations

D. M. Hoffman, H. Turner, A. Racoveanu

August 8, 2013

JANNAF Meeting 2013
Charleston, SC, United States
December 9, 2013 through December 12, 2013

Fourier Transform Rheology of Paste Explosives: I. Semtex Formulations†.

D. Mark Hoffman*, H. Turner and A. Racoveneau

High Explosives Application Facility
Lawrence Livermore National Laboratory
Livermore, CA 94550

Abstract:

Semtex 1A, H and 10 were characterized by Fourier Transform (FT) Rheology to identify the transition from linear viscoelastic to nonlinear viscoelastic behavior. Preliminary dynamic viscosities measurements on three Semtex explosives showed shear thinning behavior, typical of highly filled paste explosives. Semtex 1A and H have similar viscosity traces but 10 are less shear thinning and has lower viscosity, probably due to the different binder/plasticizer in this variant. The onset of non-linearity can be identified by a strain sweep at constant frequency when the storage and loss moduli are no longer independent of strain. The cross over point of these moduli is usually taken as the onset of fluidity. For the Semtex samples the onset of nonlinear is difficult to measure but occurs at about 0.02, 0.04 and 0.08% strain for Semtex 10, H and 1A, respectively. Based on the cross over point, Semtex 1A remains solid-like to about 7% strain, Semtex H to about 4%, but Semtex 10 is fluid-like above 0.2%. This appears to be related to the poly(acrylonitrilebutadiene) binder and different plasticizer in Semtex 10. All 3 samples had backward tilted stress and strain thinning behavior once the tests were well into the nonlinear region. Finally, transient measurements were made over a 3 order of magnitude strain sweep at 1 Hz at ambient. These results were transformed to power spectra by FT methods. The onset of nonlinearity is ascretained by the presence of higher harmonics in the power spectrum of the transient measurements. The 3^{rd} harmonic, indicating nonlinearity, was evident at above 0.01% strain in both Semtex 10 and H, but weaker at this strain in Semtex 1A.

Introduction:

The classic paste explosives, often called “plastic explosives” include C-4, PE-4, deta sheet and Semtex. They consist of 80-91% crystalline explosive, usually RDX or PETN or a mixture of both, a binder and plasticizer. Binders for these explosives include polyisobutylene (PIB), styrene-butadiene rubber (SBR) acrylonitrile-butadiene rubber (NBR) and nitrocellulose. Plasticizers include motor oil, dioctylsebacate, dioctyl phthalate, tributyl citrate or similar high boiling liquid. These explosives are the consistency of plumber’s putty or modeling clay and have a variety of military applications.[1, 2] Lower viscosity paste explosives can be formulated by reducing the concentration of explosive filler.[3] In some cases, nanoparticles have been added for gelling purposes. [3-6] Paste explosives can be cured by using a curable binder and a variety of cast-cure explosives are formulated in this way. [7-9]

----

*corresponding author hoffman2@llnl.gov

† This work performed under the auspices of the U.S. Department of Energy by Lawrence Livermore National Laboratory under Contract DE-AC52-07NA27344

Rheological behavior of these paste explosives can be quite complicated, depending on optimum particle size distribution[10] and shape[11], concentration of solids[12], type of binder and plasticizer[13]. Shear-thinning and thixotropy, shear-thickening and rheopexy and yield stresses have been observed in these types of highly concentrated suspensions. [14] Most suspensions have solids loadings below some critical solids content (ϕ_c), but paste explosives are processed so as to maximize the concentration of explosive and thereby the explosive characteristics. Recently a new method for evaluating high solids suspensions called Fourier Transform (FT) Rheology [15-17] has become available for the ARES G2 rheometer which may provide useful insight into the transition from linear viscoelastic to nonlinear viscoelastic behavior. Because of the relatively unsatisfactory results of contact angle [18], other interfacial measurements [16], and theoretical estimates[19] of the optimum binder for a given explosive crystal, an alternative approach was needed. The suggestion from some authors that large amplitude oscillatory shear (LAOS) measurements and FT rheology could provide useful information on interactions of shear induced microstructures of high solids suspensions [20-22], prompted this preliminary evaluation of the technique for the three Semtex plastic explosives.

Experimental:

Semtex samples were received in 2000 and stored at ambient without any special precautions prior to testing. Strain sweep and frequency sweep tests were run in 2010. Transient FT rheology testing was performed this year. There is some discrepancy about the compositions of the various Semtex's in the literature. [23-25] Semtex 1A is approximately 83/4/13: PETN/SBR/oil (motor oil and or phthalate). Semtex 10 is approximately 85/4/11: PETN/NBR/dibutyl formamide plasticizer. Semtex H has been reported as approximately 25/60/3/12: PETN/RDX /SBR /oil (motor oil and/or phthalate). It has also been reported to contain equal amounts of PETN and RDX.

An ARES G2® rheometer manufactured by TA Instruments was used for all tests. Frequency sweeps were run at ambient at 1% strain on a log scale from 100 to 0.1 rad/s with 10 points/decade and back to 100 rad/s. Data were acquired in correlation mode from 25 mm parallel plate fixtures with a gap of 2-3 mm. A normal force of 6-8 grams was applied to reduce slippage. The conventional strain sweeps were run at 10 rad/s on a log scale from 1E-3 to 100% strain with 5 points/decade increments at ambient. FT rheology transient measurements were run with 8 mm stainless steel serrated parallel plates to reduce slippage. Gap separation was between 2-3 mm. Axial compressive force of approximately 20 grams was maintained during transient strain sweeps. In the transient strain sweeps the strain ranged from 1E-3 to 10% with 3 points/decade. In the transient mode 5 cycles of 1028 points each were collected with a 1 second delay.

Results and Discussion:

Conventional measurements

The typical strain sweep experiment for Semtex H is shown in Figure 1a. A constant frequency (10 rad/s) was run at increasing oscillatory amplitudes from 8.7E-4% to 100% strain while various properties were measured. From the stress-strain measurements shear storage and loss moduli

(G'=blue triangles and G" green squares), tan delta (G"/G'=red diamonds) and complex viscosity (η*) were calculated. For solids nonlinear viscoelastic behavior begins when the moduli show dependence on strain.[26] From Figure 1a for Semtex H, the weak signals at low strains make the onset of nonlinearity difficult to estimate. Clearly by 0.01% strain, Semtex H moduli show some strain dependence. Similar behavior was observed in Semtex 1A and Semtex 10. At larger strains this suspensions show a cross over point between G' and G" at 3.7 % strain and 0.10 MPa. This is an indication of the transition from solid-like to liquid-like, in this case, nonlinear viscoelastic behavior.[27, 28] A second run for Semtex H (not shown) gave 6.6% strain and 0.11 MPa cross over. Semtex 1A deviated from being independent of strain around 0.006% and cross over occurred at 7.4% strain and 0.11 MPa. Semtex 10 nonlinearity onset occurred around 0.003% strain but cross over was significantly earlier at 0.4 % and 0.34 MPa. Figure 1b shows the different Lissajous figures from linear viscoelastic behavior of data point 4 to the nonlinear behavior of points 11, 16, and 22 in the strain sweep test. On the right of figure 1b are the Lissajous figures from the strain sweep in Figure 1a at 10 rad/s and 1% strain compared with similar strains and frequency in the frequency sweep in Figure 2 discussed below. The blue box in each figure shows which data points the Lissajous figures were taken from. The similarity of the 3 data sets seems to imply that transients and thixotropic behavior have equilibrated out of these data. This also implies that the nonlinear behavior in this region is reproducible.

It is possible to determine the relative magnitude of the contributions of different harmonics to the stress wave by deconvoluting the wave form and relating the various harmonic components (3, 5, 7 and 9 in Figure 2a) to the magnitude of the fundamental (1). The influence of the 3rd harmonic is seen at about 0.001% strain in the log(relative magnitude of the components of stress wave signal, I_x/I_1) plot, consistent with the deviation of the storage and loss moduli from solid-like linear viscoelastic behavior. Relative intensities below 0.001 have been ignored due to excessive scatter. The 5th harmonic begins to contribute to the resultant stress wave at strains of about 0.01%. Note also that this harmonic doesn't influence the stress wave for Semtex 1A until somewhat higher strain levels compared to the other two formulations. The 7th harmonic (red) shows up at strains above 0.04-0.05% with Semtex 1A around 0.2%. The 9th harmonic is most evident in Semtex 10 at around 0.1% strain but missing from the Semtex 1A measurements. The magnitudes of the harmonic contribution to the angular displacement signal, θ_x, are plotted in Figure 2b. Since the phase of the harmonic signal controls the shape of the composite stress wave, for structured fluids like paste explosives a peak in this function indicates a transition from a "remembered structure" to a more fluid like behavior.[29, 30] In the range tested only Semtex 10 shows this maximum, at about 25% strain, well above cross over for this explosive.

The dynamic viscosity measurements for Semtex 1A are shown in Figure 3. In the nonlinear viscoelastic region before the cross over, as was the case for both Semtex 1A and H, the storage modulus (1st run blue triangles, second run green triangles) is higher than the loss modulus and the sample behaves like a semi-solid. Both runs are reasonably similar and the stress follows the input strain with a specific delay. Dynamic viscosity traces of the 3 Semtex formulations are shown in

Figure 4. For the 3 orders of magnitude in frequency over which the tests were run, a power law relationship of the form:

$$\eta(\omega) = K\omega^{-n} \qquad (1)$$

fits the data very well. Here η is the apparent dynamic viscosity in Pa*s, ω is the oscillatory frequency in rad/s, and K and n are constants. Surprisingly, K and n values for Semtex H and 1A were very similar. Since the polymer binder and plasticizer are the same for H and 1A (SBR and oil), it is assumed that the binder/plasticizer is more important than the explosives used. This is further substantiated by the lower apparent viscosity at low frequency and reduced shear thinning character of Semtex 10. Semtex 10 uses NBR for a binder and DBF plasticizer at slightly higher PETN content.[24] Values for K and n are given in the figure.

Transient Measurements

Transient strain sweeps of the 3 Semtex explosives were performed as described in the experimental section. Figure 5a shows the measured stress for a given input strain as a function of time for Semtex H. Also shown is the strain rate (in red). The oscillating frequency was 1 Hz (6.24 rad/s). Two nonlinear (γ=0.0464% strain – measurement #6) and (γ=4.78% strain – measurement #12) transient measurements are shown in Figure 5b. The Lissajous figures from the imposed strain and measured stress are also given. As can be seen in the Figure, there is some transient damping for the first cycle or so, especially at higher strain. The nonlinearity is less easily seen at the lower strain (#6) Lissajous figure in Semtex H. Because there is an order of magnitude increase in the intensity of the harmonics when the strain is increased by two orders of magnitude, the Lissajous figure (#12) in 4b is no longer elliptical. Although the input strain (green) is sinusoidal in all instances, the stress waves (blue) are not and it is most evident in the Lissajous figures at higher strains.

The shape of the stress wave form with respect to the input sinusoidal strain depends on the phase of the harmonic components. Figure 6 shows the three Semtex stress-strain plots at a strain amplitude of 4.78%. In these figures the lag in the stress wave has been adjusted to zero so that the beginning of the wave corresponds to the sinusoidal strain oscillation. As can be seen in the figure, the Semtex 1A has a very slightly forward tilted shoulder that is almost unnoticeable. The Semtex H sample forward tilting shoulder is more pronounced at the same strain amplitude and Semtex 10 has the most predominant forward tilt. This is characteristic of concentrated suspensions prior to the onset of large viscoplastic flow.[29, 30] This happens if the phase angle of the harmonic is between 0 and 90 degrees with respect to the stress wave fundamental.[28]

The TA Instruments® a Fourier Transform Rheology package based on MIT software[31] was used to generate a power spectrum of the strain sweep data from the different Semtex samples at each different oscillation amplitude in the transient strain sweeps (see Figure 5a). An abbreviated data set for Semtex 1A with only the first of the three strain steps in a logarithmic increment is shown in Figure 7. As can be seen in the figure only the lowest strain amplitude (0.001%) shows a single fundamental or excitation frequency (harmonic number =1) with no evidence of a 3rd harmonic contribution. At 0.01 % strain, the stress wave appears to have a very small contribution from the 3rd harmonic. With increasing strain amplitude 5th and higher harmonics begin to come into play, perhaps up to the 13th. The weaker even harmonics, which should not be present, are observed at 0.1% strain and higher. According to this assessment of nonlinear effects begin around 0.01% strain. Compared to conventional measurements on Semtex 1A, the power spectrum shows significant harmonic vibrations in the stress wave at about the strain levels where the dynamic moduli begin to show strain amplitude dependence.

One method for visualization of the non-linearity of the stress wave as a function of frequency and strain amplitude is a Pipkin plot. Figure 8 shows this plot for the data generated to date on the 3 Semtex explosives. The Semtex 10 data (red traces) are in the correct position, the Semtex H data (blue) are shifted to the left and down half a log step and the Semtex 1A data are shifted down and left an order of magnitude (1 log step) for clarity. The shape change of the Lissajous figures at higher strain for Semtex 10 (red) show more dramatic changes with increasing strain amplitude and decreasing frequency than the other two Semtexs. These results can also be looked at in terms of the strain rate ($\dot{\gamma}$) which has not been done yet.

Conclusions:

A preliminary investigation into the linear to nonlinear Fourier transform rheology of the three commercial Semtex paste explosives has shown the importance of the choice of binder and plasticizer in paste formulations. It was found that the transition from linear to nonlinear behavior occurred at quite low strain amplitudes. On the other hand, the crossover in Semtex 10 occurred at an order of magnitude higher strain in the SBR/plasticizer formulations than the NBR. A maximum was observed in the harmonic phase angle with increasing strain for Semtex 10, the NBR formulation. This has been[17] associated with the transition from “strain hardening” to “viscous flow”. This peak was not observed in the A and H versions apparently because of the limit of the strain amplitude to $\leqq$ 100%. The position of this maximum might be a metric for evaluating the quality of the paste explosive. The harmonic analysis package from TA Instruments was useful in identifying early harmonic contributions in these pastes. Clearly there is much more work to be done to map out the FT rheology of paste explosives. Simple constitutive models, such as Bingham, Ellis or Carreau, have been used to aid in understanding the physical phenomena behind this interesting approach to characterizing paste and cast cure explosives. We would like to evaluate some of these simple models with respect to the FT results to obtain more physical insight into the interactions of highly loaded paste explosives in the future.

References:

1. Dobratz, B.M. and P.C. Crawford, *UCRL-52997, LLNL Explosives Handbook Properties of Chemical Explosives and Explosive Simulante*, DOE, Editor 1985, Lawrence Livermore National Laboratory: Livermore, CA. p. 1-550.
2. Meyer, R., J. Kohler, and A. Homburg, *Explosives* 5ed2002, New York, NY: Wiley-VCH. 1-424.
3. Hoffman, D.M., et al., *Transferable Insensitive Explosives (TIE)*, 1995, Lawrence Livermore National Laboratory, Livermore, CA 94550.

4. von Holtz, E., et al., *PASTE EXTRUDABLE EXPLOSIVES: THEIR HISTORY AND THEIR CURRENT STATUS*, in *ICT*1990, Franhaufer Institute: Karlsruhe, Germany.
5. Jacqueline Akhavan and Matthew R. Andrews, *Review of Paste Explosives (PEX).* Propellants Explos. Pyrotech. , 2010. **35**: p. 425-432.
6. Picart, D., R. Manceau, and J.P. Faure, *Characterization of paste-extrudable explosives using a penetration test.* Propellants Explosives Pyrotechnics, 1999. **24**(4): p. 227-231.
7. Hoffman, D.M., E.S. Jessop, and R.W. Swansiger, *RX-08-HD, A Low-Viscosity, Injection-Moldable Explosive for Filling Tortuous Paths*, 2005, UCRL-JC-127540 Preprint, Lawrence Livermore National Laboratory, Livermore, CA 94550. p. 1-23.
8. Wang, J., et al., *Preparation and Performances of Castable HTPB/CL-20 Booster Explosives.* Propellants Explosives and Pyrotechnics, 2011. **36**: p. 34-41.
9. Hoffman, D.M., et al., *LOVEX RX-35-BX, A Low-Vulnerability, High-Performance Explosive for Main-Charge Applications*, UCRL-UR-11036, Editor 1992, Lawrence Livermore National Laboratory. p. 70.
10. Erisken, C., et al., *Modeling and rheology of HTPB based composite solid propellants.* Polymer Composites, 1998. **19**(4): p. 463-472.
11. Kaully, T. and B. Keren. *Paste Explosive Based on Rounded HMX: Rheology, Sensitivity, and Mechanical properties*. in *Insensitive Munitions and Energetic Materials Technology Symposium* 2001. Bordeaux, France
12. Kohga, M. and Y. Hagihara, *Rheology of concentrated AP/HTPB suspensions prepared at the upper limit of AP content.* Propellants Explosives Pyrotechnics, 2000. **25**(4): p. 199-202.
13. BANDGAR, B.M., et al., *Mathematical Modeling of Rheological Properties of Hydroxyl-Terminated Polybutadiene Binder and Dioctyl Adipate Plasticizer.* Journal of Applied Polymer Science, 2002. **85**: p. 1002-1007.
14. Stickel, J.J. and R.L. Powell, *FLUID MECHANICS AND RHEOLOGY OF DENSE SUSPENSIONS.* Annu. Rev. Fluid Mech., 2005. **37**: p. 129-49.
15. Wilhelm, M., *Fourier-Transform rheology.* Macromolecular Materials and Engineering, 2002. **287**(2): p. 83-105.
16. Wilhelm, M., *New methods for the rheological characterization of materials.* Chemical Engineering and Processing, 2011. **50**(5-6): p. 486-488.
17. Hyun, K., et al., *A review of nonlinear oscillatory shear tests: Analysis and application of large amplitude oscillatory shear (LAOS).* Progress in Polymer Science, 2011. **36** p. 1697-1753.
18. Yeager, J.D., et al., *Adhesive properties of some fluoropolymer binders with the insensitive explosive 1,3,5-triamino-2,4,6-trinitrobenzene (TATB).* Journal of Colloid and Interface Science, 2010. **352** p. 535-541.
19. Gee, R.H., et al., *Molecular dynamics investigation of adhesion between TATB surfaces and amorphous fluoropolymers.* Macromolecules, 2007. **40**(9): p. 3422-3428.
20. Hyun, K., et al., *Large amplitude oscillatory shear as a way to classify the complex fluids.* Journal of Non-Newtonian Fluid Mechanics, 2002. **107**(1-3): p. 51-65.
21. Sim, H.G., K.H. Ahn, and S.J. Lee, *Large amplitude oscillatory shear behavior of complex fluids investigated by a network model: a guideline for classification.* Journal of Non-Newtonian Fluid Mechanics, 2003. **112**(2-3): p. 237-250.
22. Tiu, C., J. Guo, and P.H.T. Uhlherr, *Yielding, behaviour of viscoplastic materials.* Journal of Industrial and Engineering Chemistry, 2006. **12**(5): p. 653-662.
23. Hobbs, J.R., *Analysis of Semtex Explosives*, in *Advances in Analysis and Detection of Explosives, Proceedings of the 4th International Symposium on Analysis and Detection of*

Explosives, September 7-10, 1992, J. Yinon, Editor 1992, Kluwer Academic Publishers, Dordrecht, Holland: Jerusalem, Israel. p. 409.
24. Moore, S., M. Schantz, and W. MacCrehan, *Characterization of Three Types of Semtex (H, 1A, and 10).* Propellants Explos. Pyrotech. , 2010. **35**: p. 540 - 549.
25. Elbeih, A., et al., *Effect of Different Polymeric Matrices on Some Properties of Plastic Bonded Explosives.* Propellants Explosives Pyrotechnics, 2012. **37**(6): p. 676-684.
26. Franck, A.J., *APN007:Measuring and Evaluating Oscillation Data*, T. Instruments, Editor 2005.
27. Franck, A.J., *AAN031: Evaluation of nonlinear LAOS experiments*, T. Instruments, Editor 2007.
28. Franck, A.J., *APN028: Non-linear oscillation testing with the ARES-G2*, T. Instruments, Editor 2007.
29. Ewoldt, R.H. and G.H. McKinley, *On secondary loops in LAOS via self-intersection of Lissajous-Bowditch curves.* Rheologica Acta, 2010. **49**(2): p. 213-219.
30. Ewoldt, R.H., et al., *Large amplitude oscillatory shear of pseudoplastic and elastoviscoplastic materials.* Rheologica Acta, 2010. **49**(2): p. 191-212.
31. Ewoldt, R.H., P. Winter, and G.H. McKinley, *MITlaos Version 2.1 beta for MatLab*, 2007: Cambridge, MA.

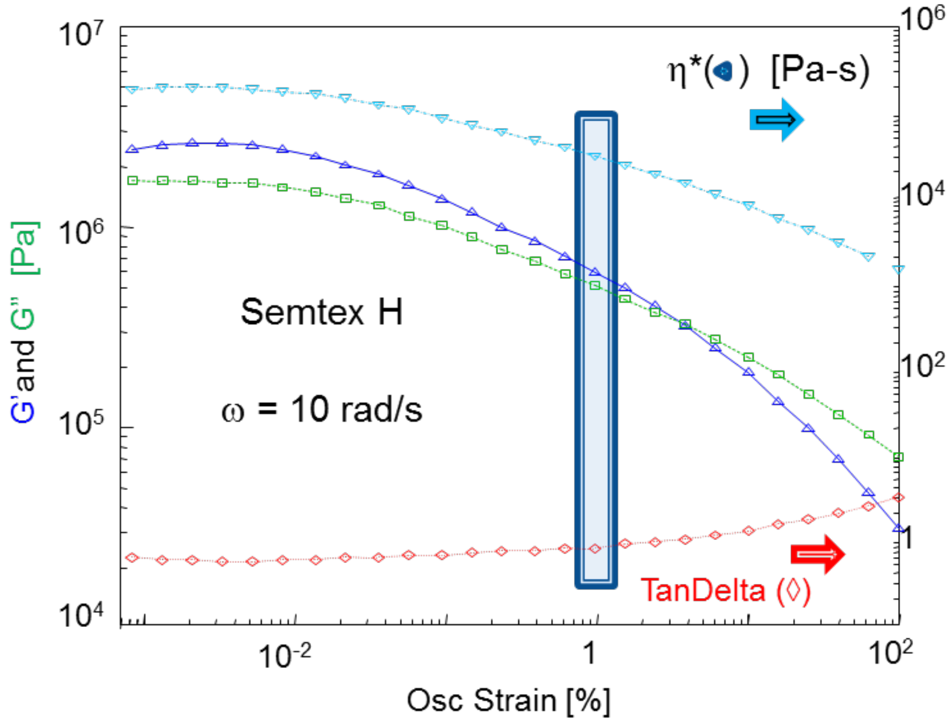

(a)

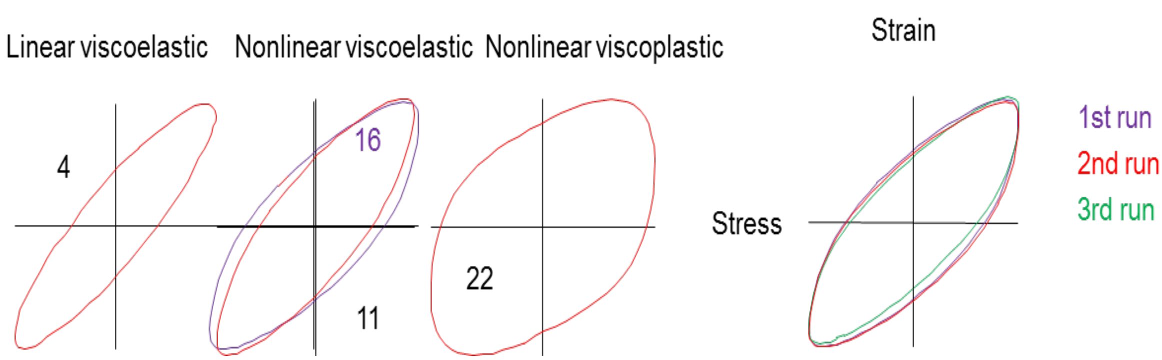

(b)

Figure 1a. Strain sweep for Semtex H shows the difficulty of identifying strain dependence in the dynamic moduli. The crossover of G' and G" indicates the onset of fluid-like behavior at 3.7 % strain and 0.10 MPa. (b) On the left are scaled Lissajous figures from normalized stress/strain data from the n^{th} data point indicated by the number in the figure. At the right three Lissajous figures from different measurement at 1 % strain and 10 rad/s are overlaid.

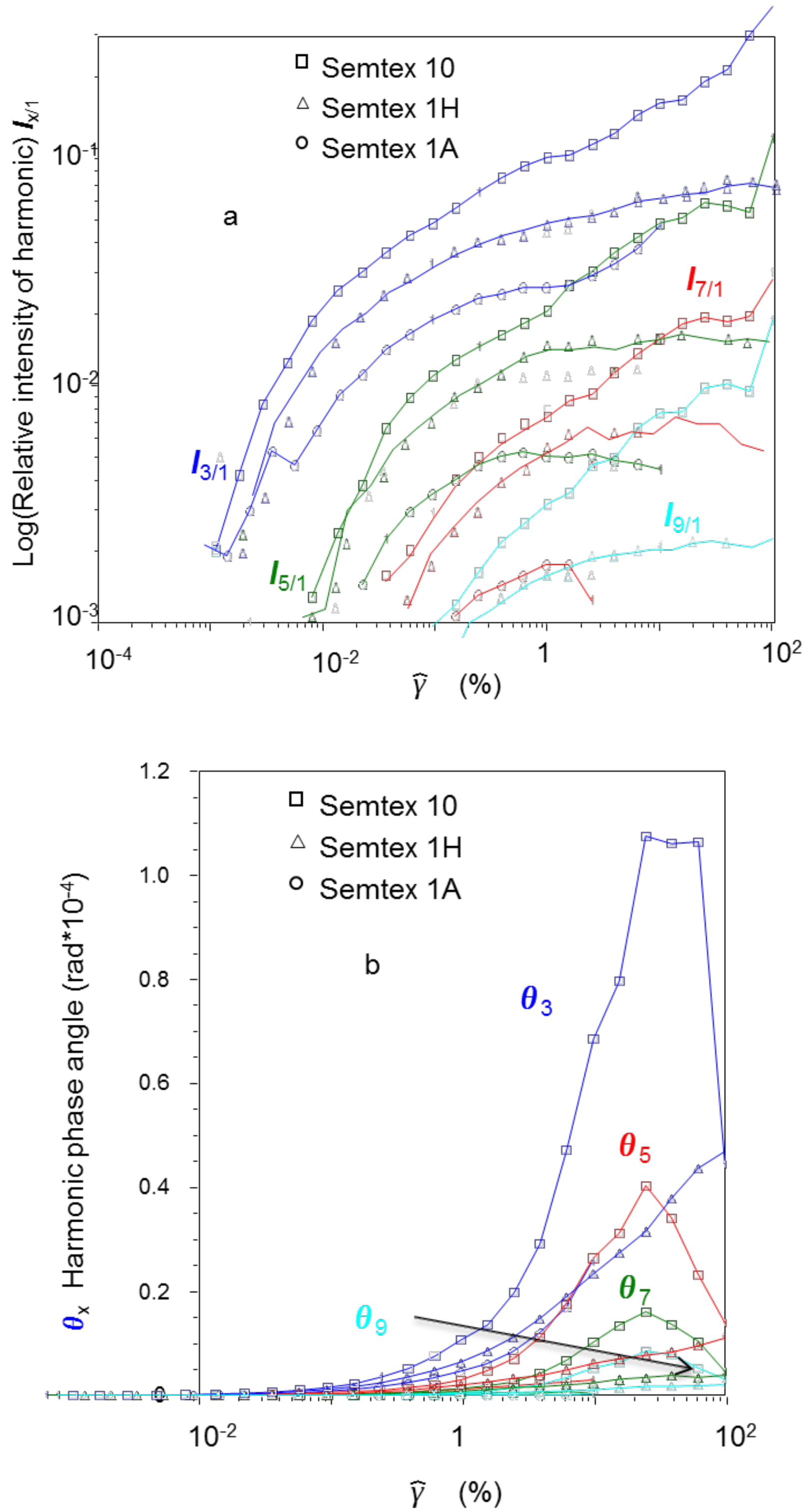

Figure 2. (a)The relative contributions of various harmonics in the stress wave were extracted from the digitized waveform and are plotted for each of the 3 Semtex variants. As expected only odd harmonics contribute and higher harmonics contribute least. (b) The harmonic phase angles of Semtex 10 pass through a maximum at about 25% strain.

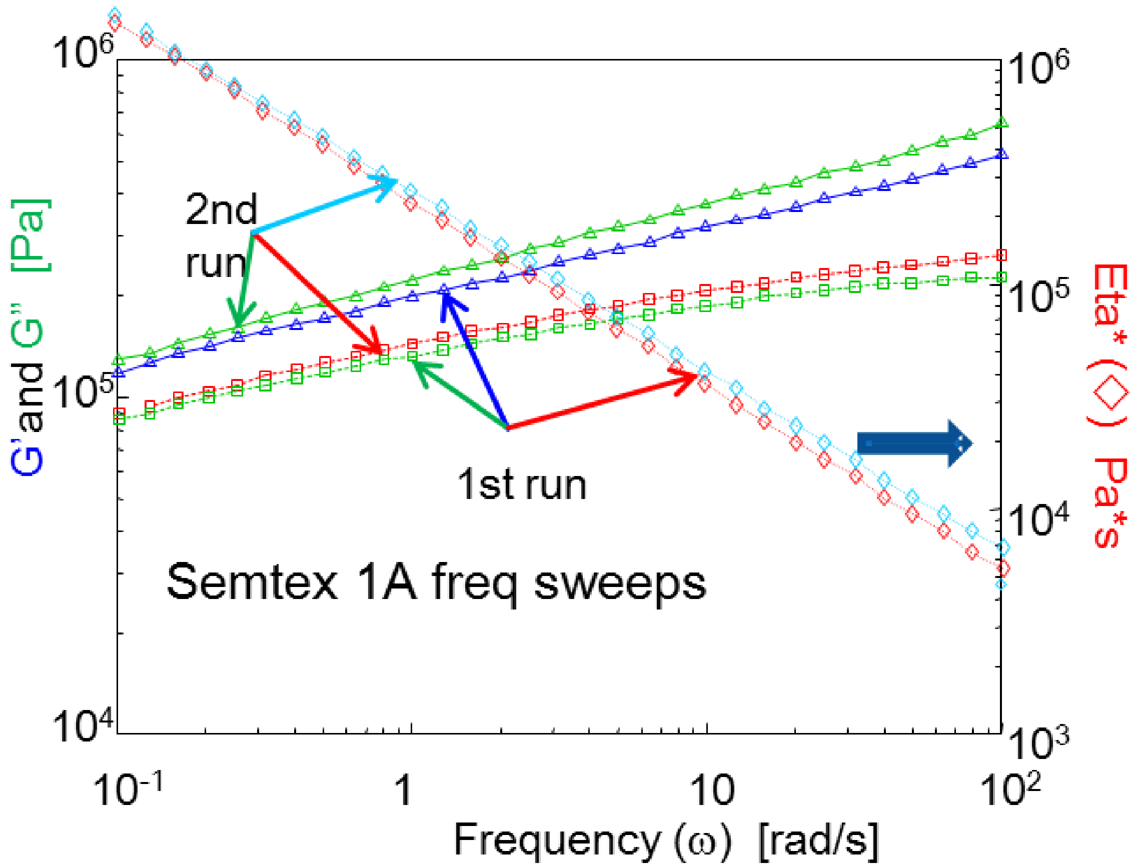

Figure 3. Typical dynamic viscosity trace for Semtex 1A with moduli included shows slight variation between first and second runs.

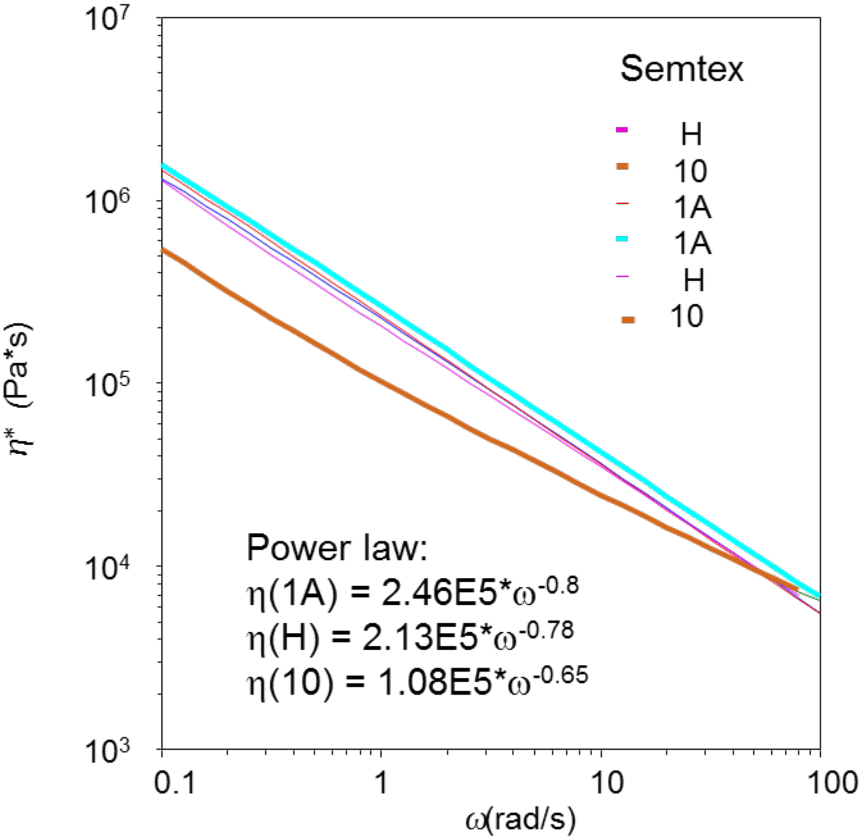

Figure 4. Dynamic viscosities of the various Semtex samples gave power law dependencies for the apparent viscosity. Semtex H and 1A were very similar but Semtex 10 was less shear thinning.

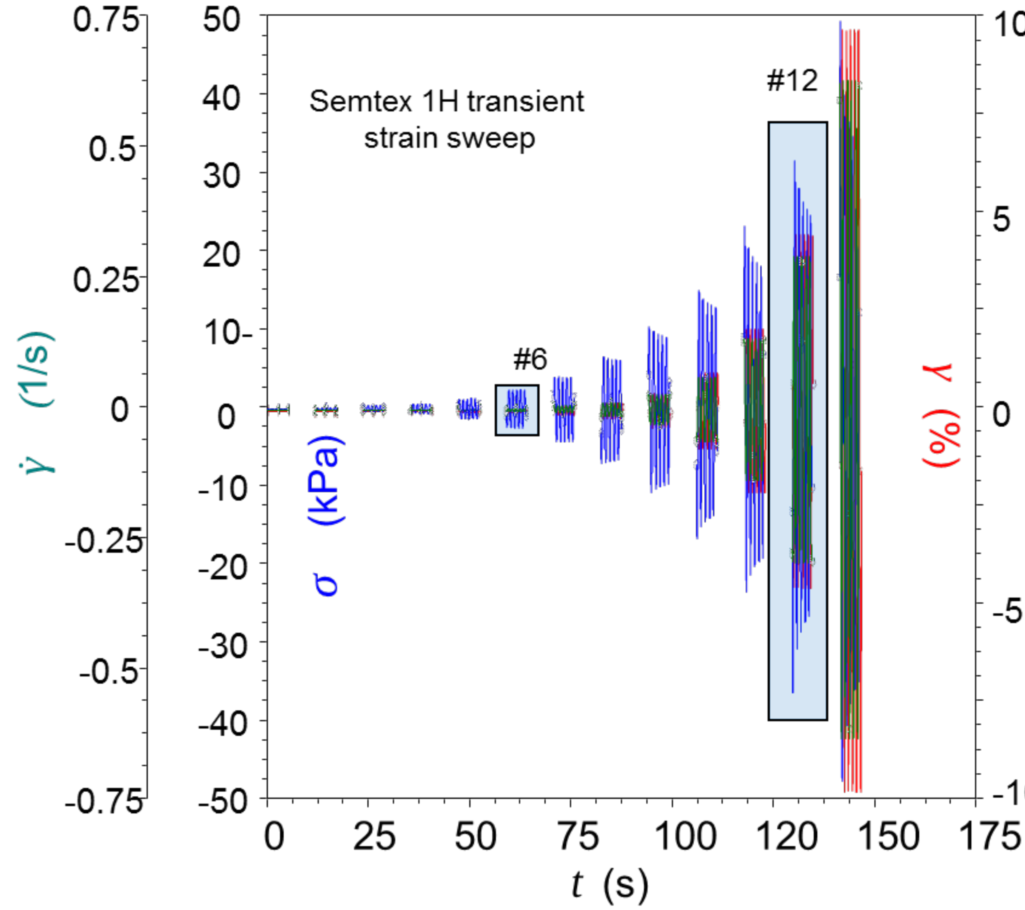

(a)

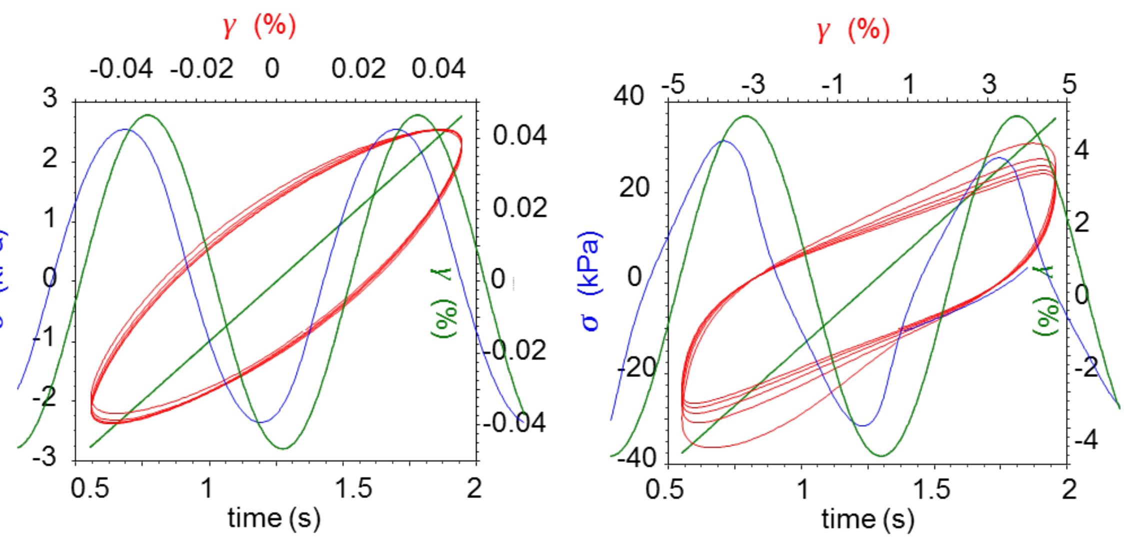

(b)

Figure 5a. (a) The transient strain sweep of Semtex H shows (b.) different degrees of nonlinear viscoelastic behavior in the stress depending on the level of imposed strain.

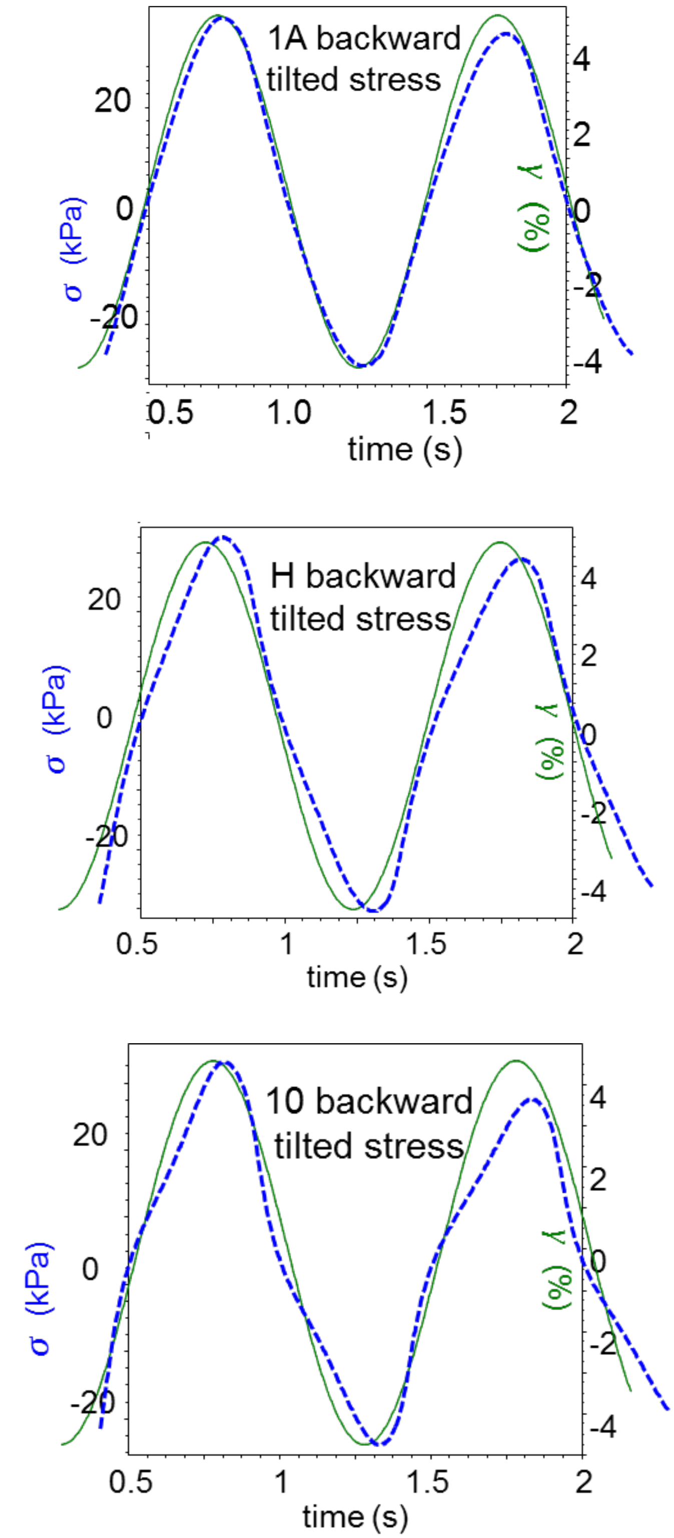

Figure 6. All of the Semtexs tested showed “backward tilting” stress waves. The strongest tilt at the 4.77% strain was with the different binder/plasticizer combination of Semtex 10.

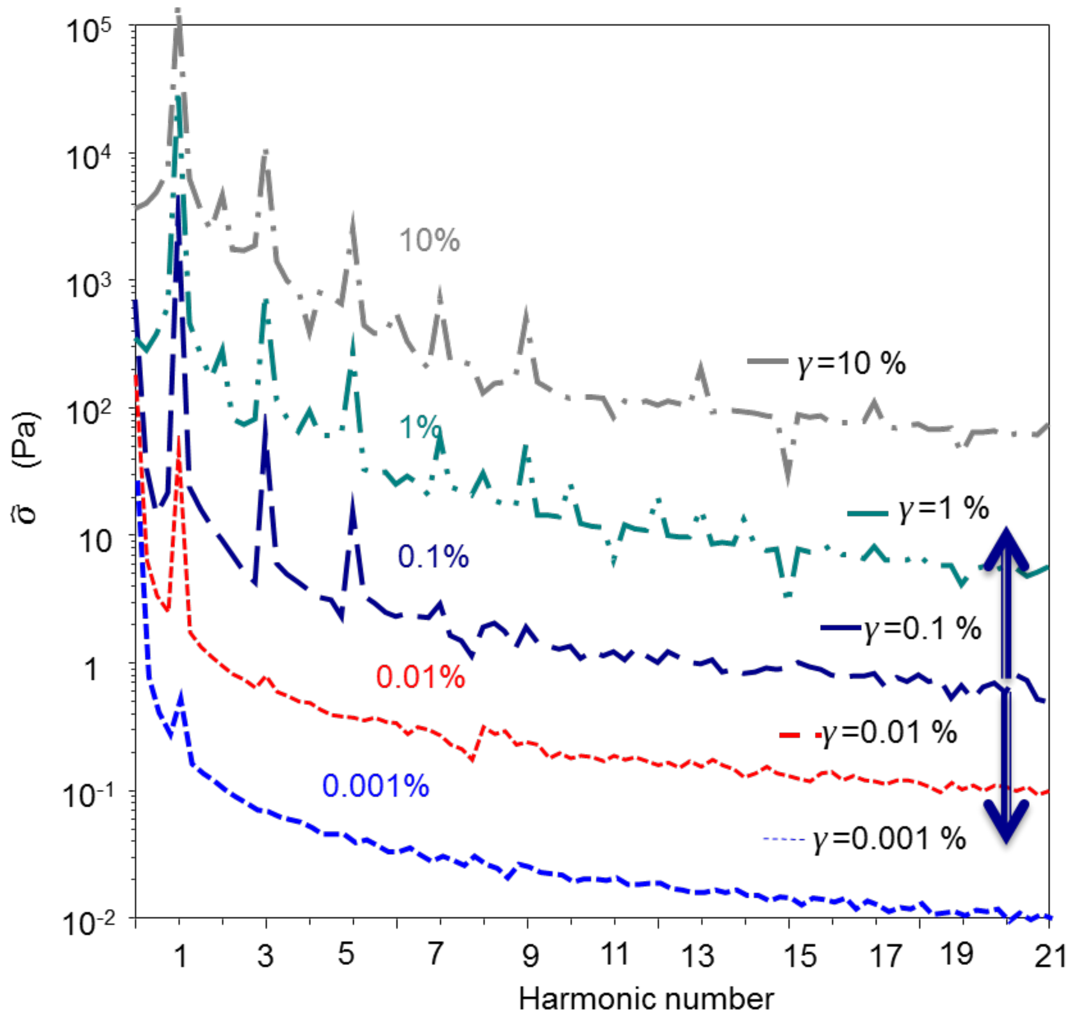

Figure 7. Fourier spectra of the Semtex 1A transient strain sweeps shifted about γ = 0.1% show increasing contributions of higher harmonics with increasing strain amplitude. Arrows indicate shift direction.

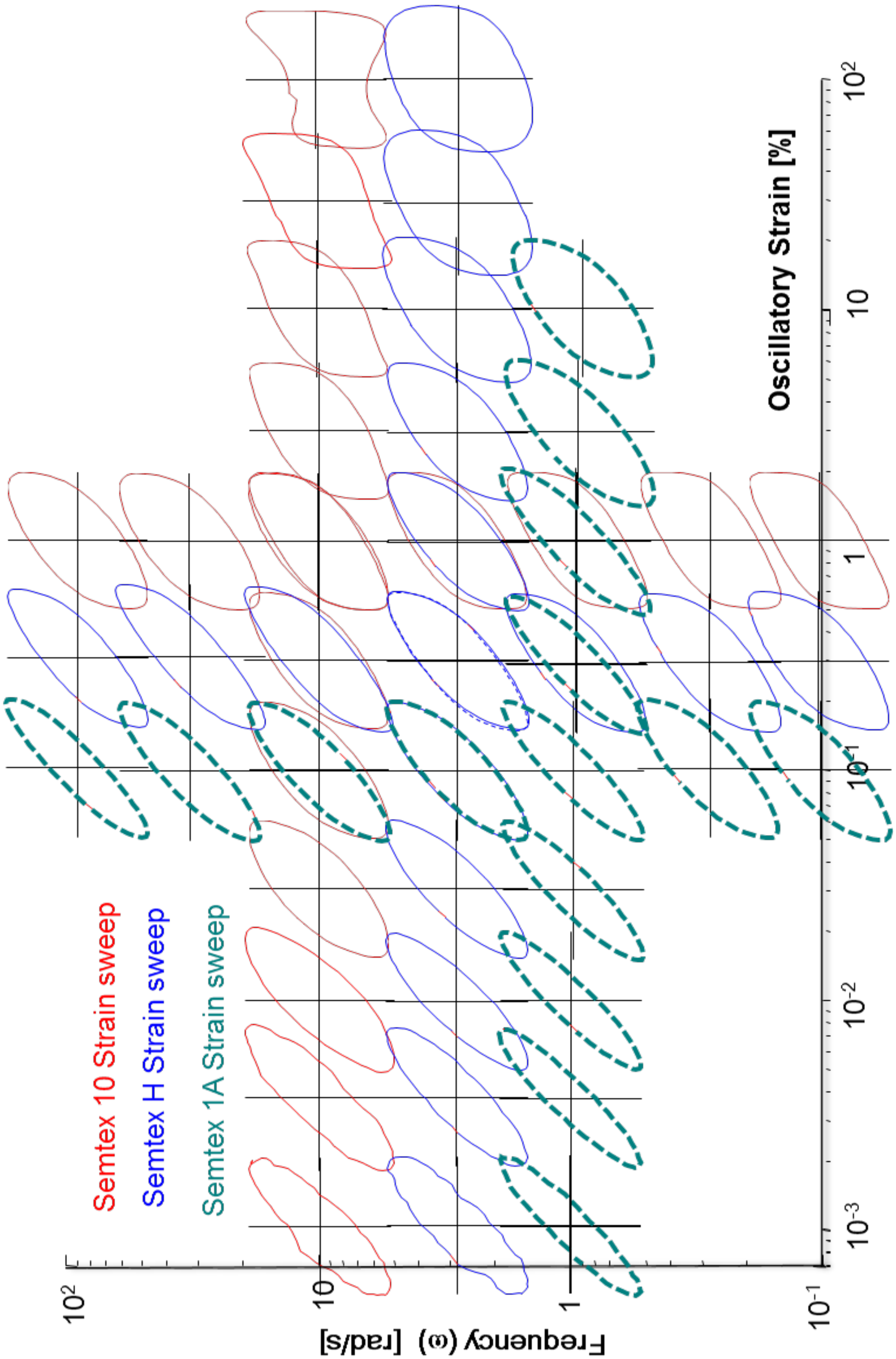

Figure 8. A subset of Pipkin plots for the 3 different Semtexs (shifted with respect to Semtex H) show that Semtex 10 nonlinearity is more pronounced than the others at higher strains.